SOPEVS: Sizing and Operation of PV-EV-Integrated Modern Homes

Anaïs Berkes
amcb6@cam.ac.uk
Department of Computer Science and Technology
University of Cambridge
United Kingdom

Srinivasan Keshav
sk18@cam.ac.uk
Department of Computer Science and Technology
University of Cambridge
United Kingdom

ABSTRACT

We address a problem that arises at the confluence of three recent trends: the popularity of storage-coupled photovoltaic (PV) systems amongst homeowners, the rapid proliferation of electric vehicles (EVs) with potential for bidirectional energy storage within PV-enabled single-family homes, and third, the surge in remote working accelerated by the Covid-19 pandemic. In this context, we explore the joint optimal sizing and operation of domestic homes while accounting for different degrees of remote working and the impact of home energy management system (HEMS) operation preferences. This task is complex due to the coupling between sizing and operation and the stochastic and non-stationary nature of solar generation, load, and EV drive cycles. We introduce SOPEVS (Sizing & Operation of PV and EV integrated Single-family homes), a novel framework formulated to tackle this multifaceted challenge. We use SOPEVS to investigate how commuting habits and choices in HEMS operation affects the sizing of domestic PV energy systems. Our findings reveal that homeowners who predominantly work from home and possess bidirectional EVs can potentially eliminate the need for separate home storage systems, thereby substantially reducing overall system costs. We also find that configuring a HEMS to maximise charging through solar energy can achieve savings of up to 80% on total system expenditure (excluding cost of EV), depending on the desired level of grid independence and the preferred State of Charge (SOC) of EV at the time of departure.

CCS CONCEPTS

• **Hardware → Energy generation and storage**.

KEYWORDS

Sizing, Operation, post-Covid, PV, Single-Family Home, Stationary Storage, WFH, HEMS, EV Charging

ACM Reference Format:

Anaïs Berkes and Srinivasan Keshav. 2024. SOPEVS: Sizing and Operation of PV-EV-Integrated Modern Homes. In *The 15th ACM International Conference on Future and Sustainable Energy Systems (E-Energy '24), June 04–07, 2024, Singapore, Singapore*. ACM, New York, NY, USA, 13 pages. https://doi.org/10.1145/3632775.3661941

E-Energy '24, June 04–07, 2024, Singapore, Singapore

ACM ISBN 979-8-4007-0480-2/24/06
https://doi.org/10.1145/3632775.3661941

1 INTRODUCTION

Climate change is an increasingly pressing issue that has had severe impacts on the environment and human populations. Deploying solar PV is a key strategy for decarbonisation, gaining significant policy support [12]. The rise in residential PV installations enhances sustainability, driven by decreasing costs of PV and battery technologies [33][22]. For example, in 2022, solar PV installations exceeded 1 GW in each of over 23 countries [2]. Despite this growth, the intermittent nature of solar power, high setup costs, and the complexity of managing small-scale systems pose ongoing challenges to broader adoption.

Energy storage is crucial for transitioning to a low-carbon economy by enabling better use of PV power through peak shifting [7]. Yet, the costs and complexities of sizing and operating storage solutions remain barriers. Interestingly, exploiting the storage capacity of EVs can boost the economic viability of PV-integrated residential houses by leveraging bidirectional charging to reduce storage needs and optimise renewable energy use [15][27]. In fact, the shift towards remote work due to the Covid-19 pandemic means EVs are parked at home for longer, enhancing their potential to be used as energy storage. This situation presents an opportunity for direct solar charging and the use of EVs as energy backup, contributing to a sustainable energy ecosystem. We explore this synergy further in this work.

Designing local distributed energy resources for modern homes presents considerable challenges, particularly when incorporating PV systems, EVs, and stationary storage (we collectively call these elements a Home Energy System (HES). A HES demands sophisticated control to enhance efficiency while ensuring resident comfort. Future designs must account for the variability of homeowner lifestyles, including work-from-home (WFH) patterns, the use of bidirectional EVs, and the benefits derived from optimised operational strategies. Existing research often overlooks these complexities, in particular, the incorporation of uni- and bi-directional EV charging and the impact of working from home and, therefore, does not provide efficient operational policies for current and future user scenarios (we discuss these challenges in greater depth in Section 3.4). Consequently, we develop a more sophisticated approach to HES design that incorporates these effects.

To confront these challenges, we introduce **SOPEVS (Sizing & Operation of PV and EV integrated Single-family homes)**, a novel framework for the integrated sizing and operation of domestic HESs, accommodating both commuting patterns and user preferences for HEMS. Permitting V2G (vehicle-to-grid technology), our framework optimises renewable energy utilisation and simultaneously reduces initial costs. Our analysis using SOPEVS explores

V2G's synergies from various work-from-home scenarios and energy management strategies, offering insights into cost-effective HES designs tailored to diverse user needs. It thus has the potential to empower modern homeowners to significantly reduce capital expenses through optimal HES design, leveraging recent shifts in commuting patterns, user preferences, and the promising capabilities of V2G technology.

We make the following contributions:

- We introduce SOPEVS, a framework for the robust and jointly optimal sizing and operation of domestic HESs incorporating PV and EV, V2G, and user WFH preferences.
- We evaluate the impact of various user commuting patterns and preferences on the configuration of PV-EV-integrated modern homes, highlighting the impact of bidirectional EVs, WFH practices, and optimised operation strategies across different user demographics.
- We demonstrate that our set of operation policies manages to generate substantial efficiency improvements by leveraging the synergy between V2G and WFH.

The remainder of this paper is laid out as follows. Section 2 surveys related work. In Section 3, we present the background to our work. Section 4 explains the SOPEVS algorithm. In Section 5, we use SOPEVS to provide insight on the impact of different user behaviours and design preferences on the sizing of residential HESs. Finally, Section 6 concludes our work and provides suggestions for future work.

2 RELATED WORK

This paper presents an algorithm for robustly and jointly optimising sizing and operation of residential HESs. It also takes into account both uni- and bi-directional EVs and the impact of working from home on EV usage patterns. We believe our work advances the field because most prior work focuses on either sizing [28] [31] or operation [18][3] of residential homes (but not simultaneously, and not in a robust fashion). Moreover, although a handful of papers do joint optimisation of sizing and operation, they do not take into account bi-directional EVs or working from home, and therefore are unable to benefit from their synergy.

We first outline common optimisation approaches, then focus on papers that do a joint optimisation of sizing and operation, and finally compare our paper with examples from prior work, showcasing the novelty of our approach.

2.1 Optimisation approaches

Four principal optimisation approaches have been reported in the literature: heuristics, mathematical optimisation, analytical algorithms and iterative simulation-based solutions.

Heuristic approaches, such as genetic algorithms [42] or particle swarm algorithms [37], can achieve fast convergence, but they may not always reach the optimal solution due to their stochastic nature. Mathematical optimisation algorithms, on the other hand, can find the optimum, but they require complex constraint equations to describe the system [6] [26]. They can also be computationally expensive since the problem is both integer and non-linear. Similarly, analytical equations also reach the exact optimal sizing solution but are difficult to formulate [5] [8] [35]. Simulation-based methods have been found to be particularly successful and efficient in optimising the robust sizing of PV systems [23]. For this reason, our work uses the simulation approach.

2.2 Joint sizing and operation

Prior work in joint sizing and operation falls into three broad categories.

The first category uses a two-stage process [32], [20], [17], [30], [29], [14]. It employs iterative techniques between investment decisions and operational dilemmas, leveraging heuristic algorithms like genetic algorithms or particle swarm optimisation. These strategies only offer near-optimal solutions and are sensitive to initial parameter settings, showing a lack of robustness to input fluctuations. Furthermore, these methods typically aim for singular objectives, like emission reduction or cost minimisation, without robust sizing guidance or addressing the complexities introduced by bidirectional EVs.

The second approach integrates planning and operation into a single optimisation process, utilising integrated techniques such as mixed-integer linear programming and fuzzy logic [6], [11]. These models are often subjective, result in lengthy computation times and are highly sensitive to specific data and parameters, limiting their capacity to offer robust sizing solutions. Furthermore, their application to complex, non-linear challenges like multi-roof sizing remains unclear, and similar to earlier methods, these approaches do not take into account EVs and the considerable efficiency improvements they can bring to the analysis.

The third approach uses a predefined operation strategies based on expert systems, where the basic rules are established [39], [43] and [4]. We use a similar approach. For instance HOMER [39], a proprietary software, allows the economical assessment and simulation of hybrid systems, while others employ genetic algorithms with predefined operating strategies [43], [4] but all of them only consider one type of expert policy, which happens to not be optimised for EV-integrated HESs.

2.3 Comparison with representative prior work

To illustrate the complex nature of the sizing and operation problem when considering PV, storage, EVs, and WFH, we compare our work with four representative papers from prior work (Table 1). Huang *et al.*. [21] present an algorithm for robustly sizing PV and storage for homes with multiple roof segments. Our work builds upon their approach, however, with several significant technical contributions, as discussed next. First, while Reference [21] also studies the sizing of solar PV and stationary storage, it does *not* consider EVs at all, let alone bidirectional EVs. Moreover, their work does not present an algorithm for joint sizing and operation, focusing only on sizing when using a simple operation policy. Lastly, it does not consider WFH patterns or other user lifestyle factors that heavily influence the sizing of solar PV and storage.

The proprietary HOMER tool [39] is widely used for optimising PV and storage. To our knowledge, it is not robust to variations in home load, nor does it consider EV load, let alone bidirectional EVs. Both Chen *et al.* [11] Mallol *et al.* [30] tackle joint sizing and operation but without considering robust optimisation, bidirectional

EVs or working from home. Chen *et al.* apply fuzzy logic to convert a dual-objective problem into a single-objective optimisation, focusing on cost and user satisfaction, Mallol *et al.* propose a dual-phase evolutionary algorithm which also does not guarantee robust outcomes.

Property	[21]	[39]	[11]	[30]	SOPEVS
Bidirectional EVs	no	no	no	no	yes
Robust	yes	no	no	no	yes
Sizing & Operation	no	yes	yes	yes	yes
WFH	no	no	no	no	yes

Table 1: Comparison of design methods for residential HESs. This table illustrates whether different properties have been demonstrated/implemented (yes) or not (no).

To sum up, our work incorporates several complex factors that are essential to model in solving the joint PV/Storage/EV sizing and operation problem. Thus, our work counts among the few that do joint sizing and operation and is the *only* one that does joint-sizing and operation in the presence of EVs, as well as bidirectional EVs. Moreover, no prior work has incorporated lifestyle elements such as WFH into the sizing decision.

3 SOLUTION APPROACH

In this section we outline our solution approach, with details in the next section.

3.1 Notation

Table 2 and Table 3 define the notation that is used in the paper.

3.2 Energy System Architecture

The grid-connected residential energy system architecture we study is shown in Figure 1. This models a typical home with multiple roof segments as in [21].

It consists of four elements: the solar PV system, stationary electrical storage, and uni- or bi-directionally charging EVs.

The PV system has a_i panels on each roof segment i, with $i \in [1, N]$, which produce a certain quantity of energy depending on the weather conditions, roof orientation, and tilt. The total solar generation of the system at time step t is given by $\sum_{i=1}^{N} S_i(t) * a_i$.

Second, an electrical storage battery buffers excess energy generation for use at a later time. Its energy content is denoted by $E^{stat}(t)$. Finally, we assume that the home has an EV that is load, but if bidirectional, can be used as additional backup storage.

The EV has a battery size of $E^{ev}_{max}(t)$ but is only charged up to the max_{SOC} level and never discharged below the min_{SOC} level. Note that SOPEVS is applicable to both uni- and bidirectional EVs.

All components are connected through DC/DC (EV, PV system) or AC/DC converters (Grid, Appliances). A HEMS handles the interactions between the components, operating with optimal control strategies that are aligned with the pre-defined user goals, see Section 4.5.

The system is operated in a grid-connected mode, meaning that load demands are guaranteed to be met, if necessary from the grid, at all times. The energy provided from the grid at time t is denoted $P_{grid}(t)$.

Symbol	Description
N	Number of roof segments
i	Index of roof segment
T	Time period over which the QoS (quality of service) criterion is computed (days)
γ	Confidence level for robustness
θ	The target upper bound in unmet energy as a fraction of overall load $\lvert L\rvert$
c_i^f	Cost of installing a panel on the ith roof segment ($)
c_i^m	Marginal cost of installing a panel on the ith roof segment ($)
c^b	Marginal cost of storage ($/kWh)
a_i^{max}	Largest possible number of panels on the ith roof segment
b^{max}	Largest possible battery size (kWh)
O	Operation policy
n	Total number of hours provided in each solar and load trace
S_i	An hourly solar power generation trace for one panel on the i^{th} roof segment; $\lvert S^i\rvert = n$
S	A vector of hourly solar power generation trace for panels on each roof segment; $S = \{S_1, ..., S_N\}$
E	An hourly EV usage trace, containing daily departure times, arrival times and SOC on arrival;
$L_{ev}(t)$	Load coming from EV charging at time step t
L	An hourly load trace (kW); $\lvert L\rvert = n$
$L[t_1, t_2]$	A subset of the load trace from time step t_1 to t_2 (kW)
$\lvert L[t_1, t_2]\rvert$	Total energy used in the load trace from time step t_1 to time step t_2 (kWh)
a_i	Number of panels, as computed by the algorithm, allocated to the ith roof segment; $0 \le a_i \le \mathcal{A}_i^{max}$
$\mathcal{A}$	The sizing, a vector of allocations $a_1, a_2, ..., a_N$
b	Size of battery, as computed by the algorithm; $0 \le b \le b^{max}$ (kWh)
u	Unmet energy for a given allocation vector, battery size, load trace, solar trace and EV trace (kWh)
T_u	Time unit, representing the number hours in each time slot t

Table 2: Table of notation for the problem formulation.

3.3 Electric Vehicle Modelling

The integration of EVs into the HES necessitates a nuanced understanding of their charging and discharging dynamics . EVs serve both as a time-varying electrical load when charging and as a potential energy storage resource when capable of bidirectional energy flow.

We model both EV and stationary storage charging and discharging processes using the model from Reference [24]. It ensures that the charging process does not surpass the desired upper SOC limit

Symbol	Description
E^{ev}_{max}	Size of the EV battery (kWh)
$E^{ev}(t)$	SOC of the EV battery at time step t(kWh)
α^{ev}_{c}	Maximum charging rate of the EV battery (kW)
α^{ev}_{d}	Maximum discharging rate of the EV battery (kW)
max_{SOC}	Maximum desired SOC ratio for the EV battery; $0 \leq max_{SOC} \leq 1$
min_{SOC}	Minimum desired SOC ratio for the EV battery; $0 \leq min_{SOC} \leq 1$
η^{ev}_{c}	Charging efficiency of the EV battery
η^{ev}_{d}	Discharging efficiency of the EV battery
a^{ev}_{1}	Lower energy limit function of the EV battery
a^{ev}_{2}	Upper energy limit function of the EV battery
$P_{net}(t)$	Net power at time step t
$P_{pv}(t)$	PV power at time step t
$P_{c}(t)$	Charging power available at time step t
$P_{d}(t)$	Discharging power available at time step t
$P^{ev}_{c}(t)$	Charging power available to the EV battery at time t
$P^{ev}_{d}(t)$	Discharging power available to the EV battery at time step t
$P_{grid}(t)$	Power drawn from the grid at time step t
$P_{dir}(t)$	Power that directly flows from the PV panels to load at time step t
$E^{stat}(t)$	Energy content of the stationary battery at time step t (kWh)
η	Number of sub-intervals sampled, for one of each a least-cost sizing is found

Table 3: Table of notation related to the operation policies, the sizing algorithm and the battery model.

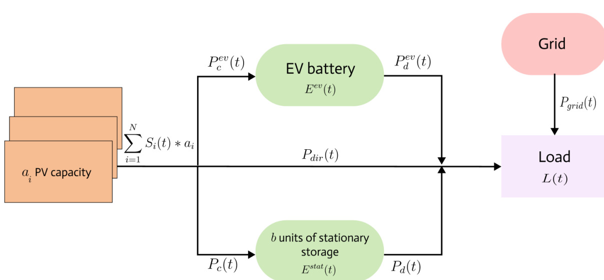

Figure 1: System Architecture

max_{SOC} , while similarly preventing the battery from being discharged below the lower SOC threshold min_{SOC}, thus preserving battery longevity.

Note that we use the terms SOC and EV battery state interchangeably, meaning that the SOC is given in kWh, while the SOC ratio is a fraction of the maximum EV capacity.

The following equations capture the charging and discharging dynamics, accounting for inefficiencies during the charging process. The battery model incrementally evaluates the energy being charged to the battery and ceases charging once it reaches the specified upper SOC limit.

This iterative procedure reflects real-world charging behaviour, ensuring that the model remains true to actual EV charging patterns.

Note that the same equations apply to the battery model of the stationary battery.

$$E^{ev}(t) = E^{ev}(t-1) + P^{ev}_{c}(t)\eta^{ev}_{c}T_u - P^{ev}_{d}(t)\eta^{ev}_{d}T_u \qquad \forall t \qquad (1)$$

$$0 \leq P^{ev}_{c}(t) \leq \alpha^{ev}_{c} \qquad \forall t \qquad (2)$$

$$0 \leq P^{ev}_{d}(t) \leq \alpha^{ev}_{d} \qquad \forall t \qquad (3)$$

$$a^{ev}_{1}(P^{ev}_{d}(t)) \leq E^{ev}(t) \leq a^{ev}_{2}(P^{ev}_{c}(t)) \qquad \forall t \qquad (4)$$

$$P^{ev}_{c}(t)P^{ev}_{d}(t) = 0 \qquad \forall t \qquad (5)$$

Equation 1 defines the energy content of the EV battery at any point in time t. Equation 2 ensures that the charge applied to the EV at time t never exceeds the user-specified maximum charging rate. Similarly, equation 3 bounds the discharge applied to the EV by the maximum discharging rate. Equation 4 assures that the energy content of the EV battery never exceeds the user-defined SOC boundaries. Lastly, equation 5 assures that the EV battery can never be charged and discharged at the same time.

Additional equations model CCCV charging and the non-linear behavior of the system near system limits [24] and have been elided for space considerations. Note that this model requires several tuning parameters: our choices are shown in Table 8 in the Appendix.

Unlike stationary batteries, the energy levels of EVs cannot be continuously accounted for, as they are only connected to the system intermittently. Thus, modelling EVs requires fine-grained traces of EV arrivals and departure times, the required state of charge (SOC) upon departure, and the timing of the next anticipated departure. Such traces are ideally sourced from EV monitoring systems that track vehicle activity. In the absence of real-world data, synthetic traces must be generated using tools such as the one presented in [9], which simulates various EV models and user behaviours, including both commuting and non-commuting patterns. We use this tool in our work.

Moreover, we assume that the HEMS will seek user input regarding anticipated departure times upon each return of the vehicle. This is vital for tailoring the charging strategy to the user's specific needs and schedules.

3.4 Why is this problem difficult?

The combination of PV, EVs and stationary batteries in a residential HES leads to a complex system that needs careful design and control to maximise efficiency and minimise cost while meeting design constraints. In part, the problem is that solar generation, residential load, and EV usage are all stochastic and non-stationary due to three effects:

- *Diurnality*: Solar irradiance is highly diurnal, as is residential load consumption, which peaks when the inhabitants are at home and using high-consumption electrical appliances. Similarly, the availability of the EV and its charging demand are also highly variable throughout the day and heavily depend on the WFH frequency. To illustrate, Figure 2 depicts these three processes for a typical homeowner who commutes to work on weekdays.
- *Seasonality*: Solar generation drops in the winter months, while load increases due to additional lighting (and, in some jurisdictions) heating demands. EV drivers tend to increase their car usage, as alternative transportation modes, such as biking and walking, become less comfortable in this period of the year.
- *Long-term trends*: Changing climates and urban landscapes, shifting commuting and vehicle usage patterns, as well as lifestyle changes all contribute to long-term changes in solar, load, and EV usage traces.

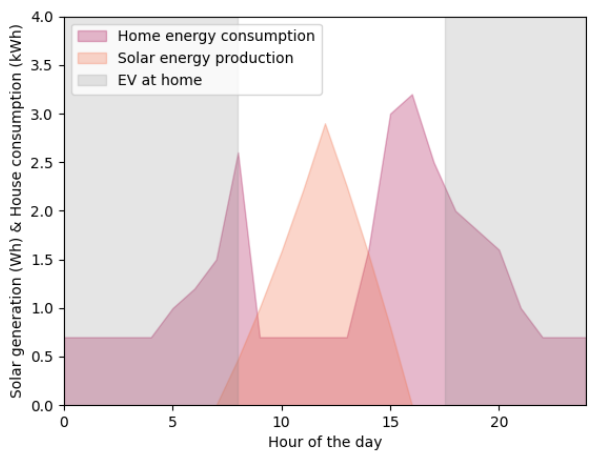

Figure 2: Shapes of the three stochastic processes: solar PV generation, load and EV presence throughout 24H for a typical commuter (WFH T1).

Given the diurnal and seasonal non-stationarity effects in solar and load data, achieving sufficient temporal resolution and duration is essential to accurately capture these changes. However, fine-grained and long-term load and EV usage data is rare. To address data limitations, we construct a circular time series from at least one year's data. This approach allows us to generate diverse future scenario samples by selecting blocks of days, ensuring a comprehensive representation of seasonal variations and long-term trends despite the well-known challenge of constrained data availability [21].

Another key challenge arises from the reliance on historical data for calculating future optimal sizing and operations, given the inherent unpredictability of future inputs. We use upper probability bounds to prevent the overfitting to historical data, as in [23]. This strategy aims to maximise robustness, reducing the sensitivity of the sizing to minor input variations (see Section 4.4).

Sizing residential HESs, even without EVs, is already a complex problem [31] and joint sizing and operation makes the problem even more challenging. Although prior work has considered this, to our knowledge, no prior work has taken EVs into account. Adding EVs to the mix greatly increases complexity since the choice of operation policies must now include both EVs and stationary storage, EVs are not always available as an energy storage, and they have a target departure SOC that must be taken into account. To tame this complexity, our approach is to pin down a handful of plausible operation policies that encompass both EVs and stationary storage. We then compute sizing for each operation policy similar to the simulation-based approach used in [21][23].

To summarize, the challenges we address in our work are as follows:

- Solar generation, residential load, and EV usage are all stochastic and non-stationary.
- We cannot rely on historical data alone for calculating future optimal sizing and operations, given the inherent unpredictability of future inputs.
- The addition of an EV to a single-family households adds a significant load to the household. It is important to make charging decisions that minimise cost and maximise PV self-consumption.
- There are many different operation policies that optimise different types of EV charging. It is thus crucial to do joint sizing and operation when sizing solar PV and storage for homes with EVs.
- If the EV supports bidirectional charging, even higher efficiency gains are possible, due to the additional storage provided while the EV is at home. Nevertheless, the EV's main goal is still to serve as a transportation mode and it is thus important that the chosen operation policy ensures relatively high SOC levels at departure times.
- Finally, different user lifestyles that directly impact the presence of the EV at home, such as WFH, can also heavily influence the operation of these retrofitted homes and therefore need to be taken into account at the design stage.

4 SOPEVS

In this section we present the details of the SOPEVS framework. The notation used in our work can be found in Table 2 and Table 3.

4.1 Inputs

SOPEVS requires the following inputs:

- Solar traces (S_i), one hourly solar trace for each roof segment i, each having n entries.
- Load trace (L) with hourly resolution and n entries.
- θ, the desired maximum ratio of load that should be met by the grid.
- γ, the desired confidence level for robustness ($0 < \gamma < 1$, with 1 being the highest confidence).
- N, the number of roof segments.
- T the time period in days over which the quality of service (QoS) criterion is computed.
- Daily EV usage trace E, including times of departure from home, times of arrival and EV SOC on arrival.

- EV battery capacity (E^{ev}_{max} in kWh).
- Maximum dis-/charging capacity of the EV (α^{ev}_c and α^{ev}_d in kWh).
- Maximum and minimum desired SOC ratio levels for the EV battery (values between 0 and 1, min_{SOC} for the lower SOC limit of the EV battery and max_{SOC} for the upper SOC limit).
- EV charging and discharging rates, α^{ev}_c and α^{ev}_d.
- Desired operation policy O, see Section 4.5.
- The cost associated to the PV modules and stationary storage: c^f_i, c^m_i and c_b.
- Maximum desired capacity for PV on each roof segment, as well as stationary storage: a^{max}_i and b^{max}.

As in prior work [21], our algorithm requires as input hourly PV generation, load traces and EV traces (S_i, L). Solar PV and load traces are accessible with devices like pyranometers or smart meters. SOPEVS can be used for any geographical region by giving the corresponding inputs for that region. Alternatively, one can acquire these traces through:

(1) Solar Traces: The NREL PVWatts calculator generates solar traces based on historical data and can simulate different traces for various roof segments by adjusting for tilt and orientation [25].
(2) Load Traces: Databases such as the one from EERE [16] offer access to load profiles. These profiles can be aligned with the target site's monthly aggregate load figures, typically found on utility bills, to approximate actual consumption patterns.

4.2 Objectives

The objective of the algorithm is to select, given the desired operation policy, the optimal number of solar panels and the appropriate amount of storage to ensure that a given load profile is satisfied with a specified QoS. A sizing that meets the QoS criterion is termed feasible. The algorithm seeks to identify the most cost-effective robust sizing that meets a target performance level with a certain statistical confidence. Specifically, given the desired operation policy O the number of roof segments N, a time period T for calculating the QoS criterion, a target unmet load ϵ, a confidence interval γ, fixed and marginal costs for the i-th solar panels c^f_i and c^m_i, marginal cost for storage c^b, the largest possible number of solar panels that can be installed on the i-th roof segment $a^{\max}_i$, the largest possible battery size $b^{\max}$, N solar traces S_i, the EV trace and the load trace L, the algorithm finds solar sizing $\mathcal{A}$ and storage sizing b such that:

- It is feasible, i.e., for all t , with probability greater than $1 - \gamma$:

$$\frac{u(\mathcal{A}, b, t, t+T)}{|L[t, t+T]|} \leq \theta$$

- It minimises the cost function[1]:

$$C(\mathcal{A}, b) = \sum_{i|a_i \neq 0} \left(c^f_i + c^m_i \times a_i\right) + \left(c^b \times b\right)$$

- The sizing is robust, i.e., it holds for future loads that are statistically similar to the past.

4.3 Constraints

In our system, the physical constraints of the components are represented through a series of equations to ensure their adherence in the simulation aspects of our algorithms. This approach aligns with the methodology outlined in [23].

$$L(t) = P_{pv}(t) + P_d(t) + P^{ev}_d(t) + P_{grid}(t) \qquad \forall t \qquad (6)$$

$$P_{pv}(t) \leq \sum_{i=1}^{N} S_i(t) a_i \qquad \forall t \qquad (7)$$

$$P_c(t) \leq P_{pv}(t) - P_{dir}(t) - L^{ev}(t) \qquad \forall t \qquad (8)$$

$$P_{dir}(t) = min(P_{pv}(t), L(t)) \qquad \forall t \qquad (9)$$

The equality Equation (6) states that the load at time t is met by the PV panels, the stationary battery, the EV battery or the grid. The equality Equation (7) constrains the available solar PV power at time t to be bounded by the solar generation of all panels on all roof segments. Equation (8) ensures that the power allocated for charging the stationary battery does not exceed the remaining available solar energy after all loads, including the EV charging load $P^{ev}_d(t)$ for certain operation policies have been satisfied. The equality Equation (9) defines the part of the load that is met directly through solar energy.

4.4 Optimisation Approach

SOPEVS extends prior work by Huang *et al.* [21], which solved the PV and storage sizing problem for multiple roofs, but without the presence of EVs and without jointly optimising sizing and operation. For completeness, we first sketch this algorithm then discuss our extensions to it.

The prior algorithm finds the minimal system configuration that meets the load while taking into account the unique characteristics of each roof segment, such as dimensions, inclination, orientation, and installation cost. Hence, SOPEVS uses the following steps:

(1) **Sampling Input Traces:** The algorithm begins by selecting η intervals from PV generation, EV usage traces and load traces to compile a series of trace tuples (S_i, L, E), serving as the data set for simulation.
(2) **Finding Minimum Cost Sizings:** For each trace tuple, the algorithm employs simulations, along with stochastic gradient descent, to determine system sizings that meet a predetermined QoS criterion, with the aim of identifying the least cost sizing for each sub-sample. The simulations assume a fixed operation policy to decide when to charge or discharge stationary storage.
(3) **Applying Multivariate Chebyshev Bound:** To ensure robustness, a statistical bound is computed for the collection of sizings, and a hyper-ellipsoid bound is established using an empirical multivariate Chebyshev method. The bound centres around the mean of the sizing set, adjusted for the

[1]We view an EV as essentially a transportation solution, rather than an energy storage solution, that has been purchased for purposes other than energy storage. From this perspective, any use of an EV as storage is 'free'. Moreover, as the EV choice is user dependent and the cost fixed once an EV choice has been made, and is independent of the sizes of solar panels and storage, we do not model this cost in our evaluations.

desired confidence level γ. The algorithm selects the most economical sizing from the upper echelon of this bound, ensuring robust system performance and cost efficiency.

We build on this algorithm in two critical ways. First, the system simulator is extended to model both stationary storage and EVs. Second, the operation policy tells the simulator how to operate both storage elements.

Specifically, at each simulation step, if the EV trace indicates that an EV is available, then, depending on the operation policy and whether the EV is uni- or bi-directional, the appropriate storage element is charged or discharged. For example, if the operation policy is N-U, there is excess PV generation over home load and the EV is not yet fully charged, the simulator would charge the EV from PV. By extending the simulator in this way, the remainder of the prior sizing algorithm proceeds without change, allowing us to convert a sizing algorithm into a joint sizing and operation algorithm that is also EV-aware. Moreover, it allows us to identify the sizing and operation policy combination that minimises cost while best satisfying user requirements. This approach ensures that each homeowner can select the operation policy and size of components that best matches their lifestyle. Indeed, the connectivity type of the EV, the WFH frequency and the user's sensitivity level to the SOC level at departure times heavily affect the final cost of the system, as demonstrated in Section 5.

4.5 Operation policies

An operation policy is used to decide when, at what rate, and the energy source (PV or grid) to use to charge either the stationary storage or the EV. Symmetrically, it decides when, at what rate, and the load to meet when discharging either the stationary storage or a bi-directional EV. Although the space of operation policies is infinite, in this work, we identify three plausible expert-designed operation policies: Naive, Solar-Only, and Solar+Grid (fully defined in Figure 3 and sketched below). These represent a spectrum of strategies ranging from the conventional, unoptimised approach prevalent among current users (Naive), through a strategy focused solely on maximising solar energy utilisation, even a the cost of not fully charging an EV (Solar-Only), to a balanced approach that seeks to optimise solar usage while ensuring a high SOC at departure times (Solar+Grid). Each paradigm applies to both unidirectional and bidirectional EVs, with the primary difference being the methodology of EV charging and discharging[2]. Importantly, the policies assume that all charging or discharging activities occur only when the EV is present at home.

The choice among these three paradigms depends on the user's preference and tolerance for uncertainty in their EV's SOC at departure times. Users must weigh their need for assurance of a fully charged EV against the potential for increased efficiency and reduced energy costs offered by the Solar-Only and Solar+Grid paradigms. This trade-off is similar to the one in Reference [10] , although in their work the goal is to flatten building load by controlling the times of EV charging.

[2]If EV battery degradation costs per charge/discharge cycle are significantly higher than for stationary batteries, then the operation policy should preferentially use stationary batteries for storing and discharging PV, relying on the EV only when the stationary battery became full/empty, since this would reduce operating costs. We do not consider this policy further in this paper.

4.5.1 *The Naive Operation Policy (N-U & N-B).*

The Naive paradigm prioritises keeping the EV as fully charged as possible, with the assumption that a departure will be known only one hour in advance. Thus, in the unidirectional Naive (N-U) policy, the EV is charged as soon as it arrives home and never discharged. In the bidirectional Naive (N-B) scenario, the EV is only discharged if the stationary battery is empty and a departure won't happen for the next hour. This reduces grid usage when possible. In both cases, charging is preferably from solar energy when it is available, and if not, then from the stationary battery, and lastly from the grid, if required.

4.5.2 *SO: The Solar-Only Operation Policy (SO-U & SO-B).*

The Solar-Only paradigm uses only surplus solar energy for EV charging, and never uses the stationary battery or the grid. In the unidirectional Solar-Only (SO-U) model, the EV is charged exclusively with remaining solar energy after domestic loads are satisfied. This approach offers no guarantees about the SOC at the next planned departure time. The bidirectional Solar-Only (SO-B) method similarly prioritises solar energy for EV charging but also allows for the use of the EV battery for discharging when the stationary battery's reserves are exhausted. Unlike N-B and SG-B, the SO-B policy doesn't consider impending departures.

4.5.3 *SG: The Solar+Grid Operation Policy (SG-U & SG-B).*

The Solar+Grid approach aims to maximise solar energy usage while ensuring high SOC levels for the EV by the next departure. This strategy broadly involves initially using available solar power for EV charging and, if necessary, supplementing it with energy from the stationary battery and grid to reach high SOC levels at expected departure times. In unidirectional systems (SG-U), excess solar energy is first directed to charge the EV, followed by the stationary battery if the EV is fully charged. In bidirectional systems (SG-B), the stationary battery is discharged first for load requirements, with EV discharge occurring only if the stationary battery is depleted and the EV does not need immediate charging due to an upcoming departure.

In summary, these paradigms offer a nuanced spectrum of EV charging strategies within HESs, allowing users to align their charging preferences with specific efficiency, reliability, and energy optimisation goals.

Figure 3 precisely defines the operation policies. The key distinction among them is the handling of the variable $L_{ev}(t)$, which is the EV charging load necessary to meet the departure SOC requirement. In the Naive paradigm, $L_{ev}(t)$ is determined at each time step t to represent the maximum feasible charging capacity for the EV battery. Conversely, in the Solar-Only approach, $L_{ev}(t)$ consistently remains at 0 across all time steps. In contrast, the Solar+Grid policy allocates a non-zero value to $L_{ev}(t)$ only when the EV's next departure is imminent and it has not yet achieved full charge.

5 EVALUATION

This section presents our experimental results, illustrates how SOPEVS can be used and demonstrates the impact of different user lifestyles and user preferences on the optimal design of PV-EV integrated HESs.

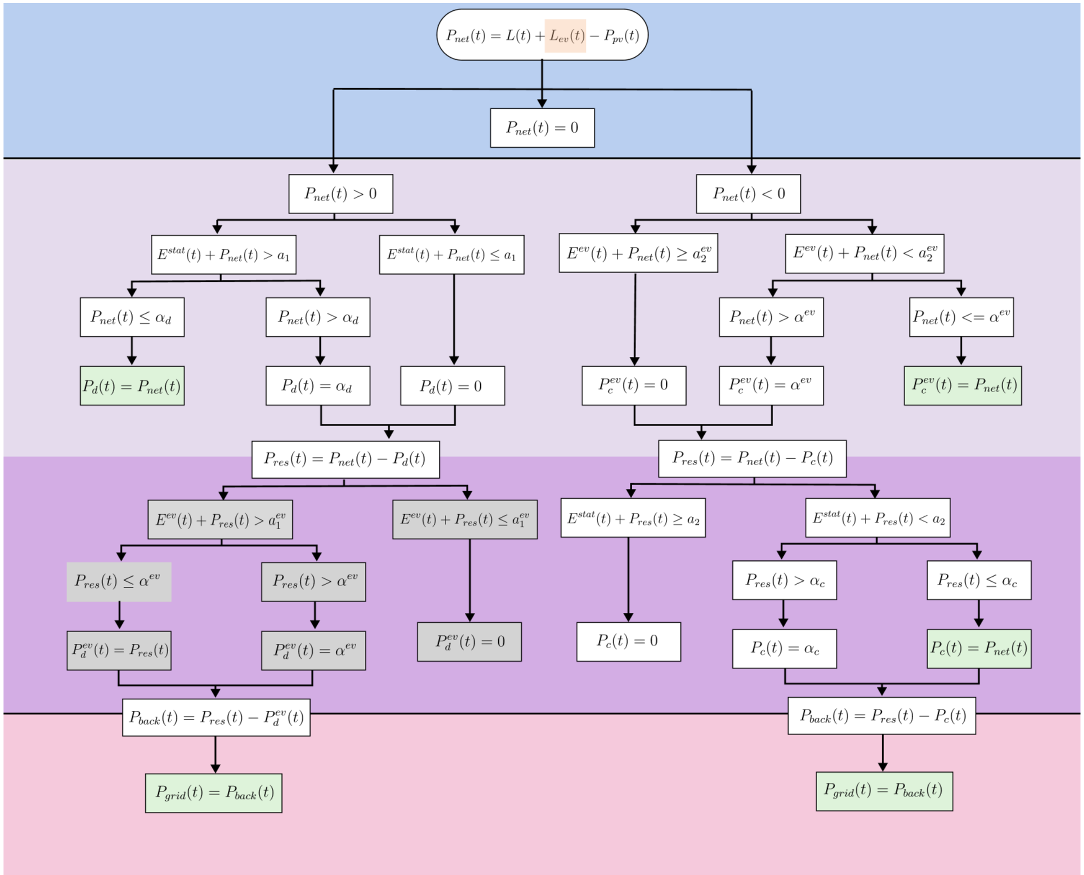

Figure 3: General power management logic that all operation policies adhere to, with variations in the value of $L_{ev}(t)$ according to the specific paradigm. The grey-shaded boxes denote steps relevant to HESs equipped with bidirectional EVs; these steps are bypassed in scenarios featuring only unidirectional EVs.

5.1 Experimental Data

SOPEVS assumes the availability of representative residential load, solar, and EV usage traces. These three data sources allow us to compute an energy system sizing that would be optimal for the given data and is robust to small variations in the inputs.

To evaluate SOPEVS and investigate the impact of various user-related parameters on the sizing of energy systems in a post-COVID world, we have modeled a realistic user setting in Austin, Texas. For the residential building load and corresponding solar traces, we use four years of data from twenty representative households from the Pecan Street Dataport dataset [1], rather than PVWatts. We select η samples from these input traces. To model EV users with different WFH frequencies and car usage patterns, we used the synthetic data generator presented in [9] to obtain representative EV drive cycles for the three most common WFH types: T1 users who commute to work with their EV on every weekday, T2 users who WFH on three days of the week and commute to work on the other two weekdays, and T3 users who always WFH.

While SOPEVS can be used to determine the optimal HES design of houses with multiple roof segments, we conducted the evaluation on single-roof homes, as the changes to the underlying simulator are identical.

In our experimental setup, we assume a marginal cost of 1250$/kW for each solar panel [38] and a battery cost of 460$/kWh, similar to the current cost of the Powerwall [34], accounting for tax credits.

We evaluate our algorithm on a confidence level of $\gamma = 0.85$, meaning that we expect the computed sizing to miss the target θ at most 15% of the time. This assumption is realistic, as we don't want to oversize our system for a few outlier load peaks in the input datasets.

Additionally, we assume a maximum roof segment solar panel capacity of $20kW$ and a maximum stationary storage capacity of $40kWh$.

Furthermore, we use a sample size of $T = 100$ days. Our baseline target for the ratio of unmet load is $\theta = 0.5$, meaning that we aim to cover at least 50% of the household's energy consumption through solar energy. Moreover, each simulation scenario starts with an empty stationary battery.

We use a Nissan Leaf with a battery size of 40 kWh [13] in our experiments. Moreover, we assume a charging and discharging efficiency of 93% [36]. We choose an upper and lower energy content limit of 80% and 20% respectively. This is done to avoid the increased wear on the battery that occurs when the cell energy content is at upper or lower extremes of the storage capacity.

As in Reference [10], the maximum at-home charging and discharging rate of the EV is set to 7.4 KW, which is common for Level-2 residential chargers.

We conduct the evaluation for all operation policies that are defined in 4.5.

5.2 Results

We study the impact of various factors on the optimal design of PV-EV integrated HESs: the choice between uni- and bidirectional EVs, the choice of the operation policy, the frequency of WFH and the desired level of grid independence.

The four main results of our experimentation with SOPEVS can be summarised as follows:

(1) Using bidirectional EVs achieves significant efficiency gains and cost reductions, particularly when coupled with a well-chosen operation policy, see Section 5.2.1.
(2) In the case of unidirectional electric vehicles, the adoption of a HEMS operation policy that optimises solar energy utilisation, coupled with a sufficient level of WFH, reduces overall costs, see Section 5.2.2.
(3) Across all results, we can see that working from home reduces both capital and operational costs, see Section 5.2.3.
(4) A high level of WFH and the SG-B policy leads to the very promising conclusion that the purchase of bidirectional EV dispenses with the need for additional home storage, see Section 5.2.4.

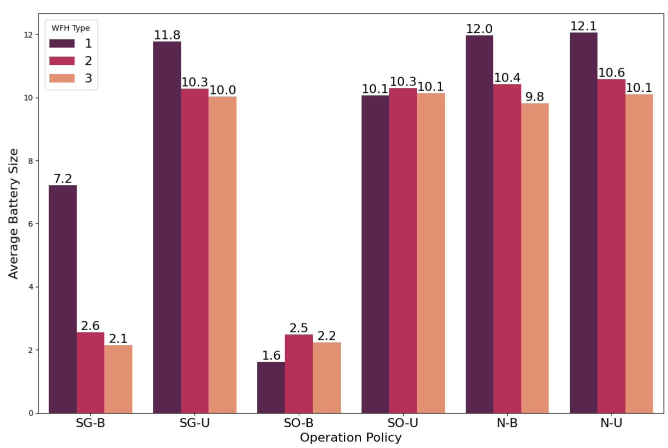

Figure 4: Battery sizes required by different operation policies and WFH types for θ = 0.5.

5.2.1 The promise of bidirectional EVs . Figure 4 shows that users with bidirectional EVs and optimised operation policies (SO-B and SG-B) require much smaller stationary batteries compared to unidirectional EV users, with bidirectional EVs achieving up to an 80% decrease in the required stationary battery size. We also see that the required stationary battery capacity for N-B users is roughly the same as for all homeowners with unidirectional EVs, proving that it does not pay off to purchase a bidirectional EV when using a naive operation policy.

Bidirectional EVs can entirely eliminate the need for stationary batteries in some cases, as can be seen in Table 5. For instance, homeowners looking to meet at most 80% of their electricity load from the grid, can neglect the stationary battery if they implement the SG-B policy. Similarly, a homeowner looking to meet at most 50% of their electricity load from the grid, can neglect the stationary battery if they use the SO-B policy. Clearly, using SO-B leads to the highest cost savings across all WFH frequencies and levels of θ (see Table 9 and Table 10). This is mainly due to the significant decrease in stationary battery needs. Nevertheless, SG-B also achieves significant cost reductions, between 12% and 45%, with higher savings achieved for higher WFH frequencies and higher grid independence levels.

While the SO-B policy achieves the lowest overall costs across all WFH types, it is not optimal if the user is sensitive to the SOC at departure, as can be seen in Figure 5 and Table 4: the average SOC at departure for SO-B is much lower than that for the other policies, with 15.7 kWh being far less than the SOC goal of 32 kWh (80% of the total battery capacity). This trend is even worse for users who work more from home, see Figure 6 and Figure 7 for T2 and T3 users. Table 4 also shows that the probability of missing the SOC target of 32 kWh by over 30% or even by over 50% is quite high for SO-B across all WFH types. It is unlikely that most homeowners will be comfortable with this risk level, even if SO-B leads to the highest overall cost decrease among all operation policies.

Interestingly, Figure 5 shows that the SG-B operation policy achieves a relatively high average SOC on departure, with 30.5 kWh on average for T1 users and even higher results for T2 (30.97 kWh, see Figure 6) and T3 users (31.04 kWh, see Figure 7). In addition, using SG-B leads to a very low, almost negligible, probability of falling below 30% of the SOC goal, as can be seen in Table 4, making it a safe operation policy choice for most homeowners. Moreover, Figure 4 proves that SG-B still achieves competitive results, especially for T2 and T3 users. As a result, SG-B provides the advantage of maintaining a relatively high SOC of the EV at the departure time, while still achieving significant cost reductions.

Table 4: Probabilities that the average SOC misses the target SOC value by more than 30% and more than 50% for T1 users.

HEMS	WFH	> 30% SOC deficit	> 50% SOC deficit
SG-B	T1	0.05	0.03
SO-B	T1	0.67	0.41
SG-B	T2	0.03	0.01
SO-B	T2	0.83	0.69
SG-B	T3	0.03	0.01
SO-B	T3	0.78	0.60

5.2.2 Optimising HESs with unidirectional EVs . We now study how to reduce costs even in HESs that only have access to unidirectional

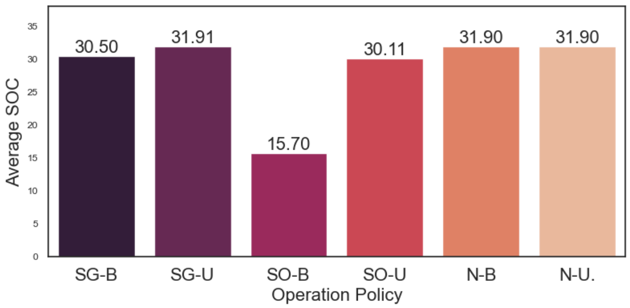

Figure 5: Average SOC at departure from home for T1 commuters and the different operation policies.

EVs, which is still the standard nowadays. Figure 4 shows that some battery capacity reductions of about 2kWh are achievable through the use of SG-U or SO-U. This shows that optimising the operation policy for unidirectional EVs leads to efficiency gains, but that they are, by far, not as significant as with bidirectional EVs.

Still, it is advisable for unidirectional EV users to use the SG-U or even the SO-U policies in their HEMS, as they never reach dangerously low SOC levels around departure times, with their probability of missing the target SOC by more than 30% being 0.0. Moreover, the average SOC on departure for the SG-U and SO-U policies (31.91 kWh and 30.11 kWh respectively for T1, see Figure 5) is very close to the desired SOC level of 32 kWh. The surprising result for SO-U in Figure 5 underlines that even homeowners who commute to work every day can still reach high enough SOC levels by charging their EV *only* from solar energy, at least in this study setting.

Additionally, Table 5 demonstrates that using the SO-U operation policy can lead to important savings, ranging from 8% to 31% and depending on the desired level of grid independence and the WFH type, with higher results achieved for higher commute levels, see Table 9 and Table 10.

Thus, homeowners with unidirectional EVs who WFH on some days and use the SO-U paradigm in their HEMS can achieve significant cost reductions. This is especially true for users who commute more (T1). We, therefore, encourage typical EV commuters to use the SO-U policy in their HEMS systems and to consider increasing their WFH frequency to achieve significant cost reductions.

5.2.3 The benefits of WFH . We now demonstrate that it pays off to work from home for two to three days each week. In fact, Figure 4 displays a significant reduction in the required battery capacity if a user switches from a T1 to a T2 WFH lifestyle, this jump is especially important for homeowners with a SG-B system, with a battery capacity reduction of more than 60%. Conversely, increasing the WFH frequency from three WFH days (T2) to a full WFH mode (T3) does not lead to any significant savings, as these two types have very similar stationary battery requirements across the different operation policies. Moreover, even if a T1 homeowner does not optimise their HEMS at all and uses the N-U policy, they can already achieve a 10% system cost reduction only by increasing their WFH frequency, and even more important savings if they optimise their operation policy, as can be seen in Table 6.

θ	HEMS	PV (kW)	Battery (kWh)	Cost ($)	Savings
0.8	N-U	2.25	2.94	4162	Baseline
	SG-U	2.27	2.47	3978	-4%
	SO-U	1.77	1.44	2875	-31%
	N-B	2.25	2.82	4117	-1%
	SG-B	1.89	1.16	2901	-30%
	SO-B	0.77	0.04	976	-77%
0.5	N-U	4.60	12.06	11297	Baseline
	SG-U	4.56	11.78	11120	-2%
	SO-U	4.11	10.06	9763	-14%
	N-B	4.62	11.98	11283	-0%
	SG-B	4.46	7.21	8904	-21%
	SO-B	1.61	0.99	1982	-83%
0.2	N-U	7.82	26.76	22095	Baseline
	SG-U	7.70	26.61	21862	-1%
	SO-U	7.23	24.67	20393	-8%
	N-B	7.75	26.67	21962	-0.6%
	SG-B	7.54	22.06	19575	-12%
	SO-B	3.69	5.73	7257	-67%

Table 5: Sizing results obtained with SOPEVS for different θ values and operation policies for WFH T1 users, with the cost decrease compared to the baseline operation policy N-U.

WFH	HEMS	PV (kW)	Battery (kWh)	Cost ($)	Savings
T1	N-U	4.60	12.06	11297	Baseline
	SG-U	4.56	11.78	11120	-2%
	SO-U	4.11	10.06	9763	-14%
	N-B	4.62	11.98	11283	-0%
	SG-B	4.46	7.21	8904	-21%
	SO-B	1.61	0.99	1982	-83%
T2	N-U	4.29	10.57	10222	-10%
	SG-U	4.23	10.28	10018	-12%
	SO-U	4.14	10.29	9905	-13%
	N-B	4.30	10.41	10169	-10%
	SG-B	4.16	2.55	6373	-44%
	SO-B	1.68	2.49	3242	-72%
T3	N-U	4.09	10.09	9762	-14 %
	SG-U	4.08	10.03	9716	-14%
	SO-U	4.03	10.14	9697	-14%
	N-B	4.05	9.81	9580	-15%
	SG-B	3.62	2.15	5515	-51%
	SO-B	3.07	2.23	4858	-57%

Table 6: Sizing results obtained with SOPEVS for different WFH types and operation policies for $\theta = 0.5$ and cost decrease compared to the baseline case of N-U & T1.

WFH	HEMS	EV_c	EV_d	Stat_c	Stat_d
T1	N-U	1.5	0	5.4	3.9
	SG-U	1.3	0	4.2	2.5
	SO-U	0.1	0	4.1	2.5
	N-B	2.8	1.4	5.4	3.9
	SG-B	6.5	3.0	3.0	1.8
	SO-B	0.1	4.0	0.1	0.1
T2	N-U	0.4	0	4.5	3.0
	SG-U	0.3	0	4.2	2.5
	SO-U	0.2	0	4.1	2.5
	N-B	1.8	1.6	4.5	2.9
	SG-B	7.4	4.1	0.6	0.3
	SO-B	0.6	3.7	0.1	0.1
T3	N-U	0.1	0	4.1	2.6
	SG-U	0.1	0	4.1	2.6
	SO-U	0.1	0	4.1	2.6
	N-B	1.6	1.8	4.1	2.5
	SG-B	5.5	3.5	0.2	0.1
	SO-B	3.3	3.1	0.1	0.1

Table 7: Average daily number of kWh charged and discharged in the EV and stationary batteries (rounded to one decimal place).

5.2.4 The powerful synergy of WFH and SG-B . Lastly, we emphasize that a combination of some degree of WFH with the use of bidirectional EVs can lead to very promising efficiency gains. Table 6 displays the savings that can be achieved by choosing an optimised operation policy and increasing the WFH level compared to the typical T1 user who uses the N-U policy. For instance, working from home and using the SG-B policy can reduce the required stationary battery size by a factor of 5 and therefore reduce the total system cost by 44%. Even higher savings (up to 72%) can be achieved by using the SO-B policy or by further increasing the WFH frequency, but the additional savings obtained from only working from home are not as significant. Additionally, using the SO-B policy comes with a high risk of low SOC levels, as we have seen in Table 4 and Figure 5.

Moreover, Table 7 illustrates that the average quantity of kWh discharged from the EV battery represents only a small fraction of its total capacity and does therefore not substantially accelerate battery degradation [41][40][19].

Thus, we recommend two to three WFH days (T2) and the use of the SG-B as an optimal combination, as this guarantees high EV battery SOC levels on departure times, while still achieving a cost reduction of more than 40%.

Table 5, Table 9 and Table 10 demonstrate that all cost reduction trends are visible across all choices of θ and thus do not dependent on the desired level of grid independence. More grid independence generally just results in higher stationary battery capacity requirements. It is also the variation in the stationary battery size that lies behind most of the cost savings that can be achieved by more optimised operation policies (SG-B, SO-U), as the recommended PV size stays relatively stable across policies for a chosen level of θ.

Conclusively, we find that there are many opportunities for different homeowners to improve their HES designs by choosing their right combination of WFH level and operation policy.

6 CONCLUSION

We introduce SOPEVS, a novel framework for the joint sizing and operation of PV-EV-integrated domestic HESs. Extending a prior algorithm for solar and storage sizing to account both for EVs and differing operation policies, we used a data-driven and simulation-based approach to study the synergy between working from home and bidirectional EVs in energy system sizing and operation, which we believe to be novel. We find that working from home tends to reduce system cost and that when combined with an optimised bidirectional operation policy, it can entirely dispense of stationary storage. We also find that configuring a HEMS to maximise charging through solar energy can achieve savings of up to 80% on total system expenditure, depending on the desired level of grid independence and the preferred SOC of EV at the time of departure.

Our work highlights the importance of personalising sizing and operation to account for variables such as work from home frequency, commute distance, and user preferences, which is absent from prior work. We find that optimal microgrid design requires a nuanced approach, factoring in individual lifestyles and preferences to maximise benefits.

While our work has its limitations, such as the reliance on predefined operation strategies, our findings, we believe, pave the way for more sustainable, efficient, and personalised residential energy systems. Key research areas that would significantly augment this study include examining time-dependent grid independence and integrating grid tariffs into the optimisation process. These topics present valuable directions for future research.

REFERENCES

[1] 2023. *Pecan Street Dataport.* https://dataport.pecanstreet.org

[2] International Energy Agency. 2023. *Snapshot of Global PV Markets 2023.*

[3] Saad Ahmad, Md Shafiullah, Chokri B Ahmed, and Maad Alowaifeer. 2023. A Review of Microgrid Energy Management and Control Strategies. *IEEE Access* (2023).

[4] Amirsaman Arabali, Mahmoud Ghofrani, Mehdi Etezadi-Amoli, and Mohammed Sami Fadali. 2013. Stochastic performance assessment and sizing for a hybrid power system of solar/wind/energy storage. *IEEE Transactions on Sustainable Energy* 5, 2 (2013), 363–371.

[5] P Arun, Rangan Banerjee, and Santanu Bandyopadhyay. 2010. Optimum design of diesel generator integrated photovoltaic-battery system. *Energy & fuels* 24, 12 (2010), 6565–6575.

[6] Raji Atia and Noboru Yamada. 2016. Sizing and analysis of renewable energy and battery systems in residential microgrids. *IEEE Transactions on Smart Grid* 7, 3 (2016), 1204–1213.

[7] Sarah Paul Ayeng'o, Toni Schirmer, Kai-Philipp Kairies, Hendrik Axelsen, and Dirk Uwe Sauer. 2018. Comparison of off-grid power supply systems using lead-acid and lithium-ion batteries. *Solar Energy* 162 (2018), 140–152.

[8] Santanu Bandyopadhyay. 2011. Design and optimization of isolated energy systems through pinch analysis. *Asia-Pacific Journal of Chemical Engineering* 6, 3 (2011), 518–526.

[9] Anaïs Berkes and Srinivasan Keshav. 2024. SPAGHETTI: a synthetic data generator for post-Covid electric vehicle usage. *Energy Informatics* 7, 1 (2024), 1–21.

[10] Harsimrat Singh Bhundar, Lukas Golab, and Srinivasan Keshav. 2023. Using EV charging control to provide building load flexibility. *Energy Informatics* 6, 1 (2023), 5.

[11] Jian Chen, Weitong Zhang, Jiaqi Li, Wen Zhang, Yutian Liu, Bo Zhao, and Yicheng Zhang. 2017. Optimal sizing for grid-tied microgrids with consideration of joint optimization of planning and operation. *IEEE Transactions on Sustainable Energy* 9, 1 (2017), 237–248.

[12] Hans Christoph Curtius. 2018. The adoption of building-integrated photovoltaics: barriers and facilitators. *Renewable Energy* 126 (2018), 783–790.

[13] Electric Vehicle Database. 2022. *Nissan Leaf.* https://ev-database.org/uk/car/1656/Nissan-Leaf
[14] Maria Luisa Di Silvestre, Giorgio Graditi, and Eleonora Riva Sanseverino. 2013. A generalized framework for optimal sizing of distributed energy resources in micro-grids using an indicator-based swarm approach. *IEEE Transactions on Industrial Informatics* 10, 1 (2013), 152–162.
[15] Mehrdad Ehsani, Milad Falahi, and Saeed Lotfifard. 2012. Vehicle to grid services: Potential and applications. *Energies* 5, 10 (2012), 4076–4090.
[16] U.S. DEPARTMENT OF ENERGY. 2024. *Open Energy Data Initiative.* https://data.openei.org
[17] Samira Fazlollahi, Pierre Mandel, Gwenaelle Becker, and Francois Maréchal. 2012. Methods for multi-objective investment and operating optimization of complex energy systems. *Energy* 45, 1 (2012), 12–22.
[18] Kaiye Gao, Tianshi Wang, Chenjing Han, Jinhao Xie, Ye Ma, and Rui Peng. 2021. A review of optimization of microgrid operation. *Energies* 14, 10 (2021), 2842.
[19] Jingyu Gong, David Wasylowski, Jan Figgener, Stephan Bihn, Fabian Rücker, Florian Ringbeck, and Dirk Uwe Sauer. 2024. Quantifying the impact of V2X operation on electric vehicle battery degradation: An experimental evaluation. *eTransportation* 20 (2024), 100316.
[20] Li Guo, Wenjian Liu, Jiejin Cai, Bowen Hong, and Chengshan Wang. 2013. A two-stage optimal planning and design method for combined cooling, heat and power microgrid system. *Energy Conversion and Management* 74 (2013), 433–445.
[21] Brad Guanqiao Huang, Fiodar Kazhamiaka, and Srinivasan Keshav. 2021. Sizing Solar Panels and Storage for Multiple Roofs. In *Proceedings of the Twelfth ACM International Conference on Future Energy Systems.* 84–94.
[22] J. Skea R. Slade A. Al Khourdajie R. van Diemen D. McCollum M. Pathak S. Some P. Vyas R. Fradera M. Belkacemi A. Hasija G. Lisboa S. Luz J. Malley (eds.) IPCC, P.R. Shukla. 2022. Climate Change 2022: Mitigation of Climate Change. Contribution of Working Group III to the Sixth Assessment Report of the Intergovernmental Panel on Climate Change. (2022).
[23] Fiodar Kazhamiaka, Yashar Ghiassi-Farrokhfal, Srinivasan Keshav, and Catherine Rosenberg. 2019. Comparison of different approaches for solar PV and storage sizing. *IEEE Transactions on Sustainable Computing* 7, 3 (2019), 499–511.
[24] Fiodar Kazhamiaka, Catherine Rosenberg, Srinivasan Keshav, and Karl-Heinz Pettinger. 2016. Li-ion storage models for energy system optimization: the accuracy-tractability tradeoff. In *Proceedings of the Seventh International Conference on Future Energy Systems.* 1–12.
[25] National Renewable Energy Laboratory. 2024. *PVWatts Calculator.* https://pvwatts.nrel.gov
[26] Chun Sing Lai and Malcolm D McCulloch. 2016. Sizing of stand-alone solar PV and storage system with anaerobic digestion biogas power plants. *IEEE Transactions on Industrial Electronics* 64, 3 (2016), 2112–2121.
[27] Paolo Lazzeroni, Sergio Olivero, Maurizio Repetto, Federico Stirano, and Marc Vallet. 2019. Optimal battery management for vehicle-to-home and vehicle-to-grid operations in a residential case study. *Energy* 175 (2019), 704–721.
[28] Shalom Irence LB and A Immanuel Selvakumar. 2021. Optimal Sizing of Various Types of Microgrids-A Review. *Journal of Engineering Science & Technology Review* 14, 6 (2021).
[29] Mingtao Ma, Huijun Huang, Xiaoling Song, Feniosky Peña-Mora, Zhe Zhang, and Jie Chen. 2022. Optimal sizing and operations of shared energy storage systems in distribution networks: A bi-level programming approach. *Applied Energy* 307 (2022), 118170.
[30] R Mallol-Poyato, S Jiménez-Fernández, P Díaz-Villar, and S Salcedo-Sanz. 2016. Joint optimization of a Microgrid's structure design and its operation using a two-steps evolutionary algorithm. *Energy* 94 (2016), 775–785.
[31] Mobi Mathew, Md Shafayet Hossain, Sajeeb Saha, Som Mondal, and Md Enamul Haque. 2022. Sizing approaches for solar photovoltaic-based microgrids: A comprehensive review. *IET Energy Systems Integration* 4, 1 (2022), 1–27.
[32] Mohammad H Moradi, Mohsen Eskandari, and S Mahdi Hosseinian. 2014. Operational strategy optimization in an optimal sized smart microgrid. *IEEE Transactions on Smart Grid* 6, 3 (2014), 1087–1095.
[33] Eric O'Shaughnessy, Dylan Cutler, Kristen Ardani, and Robert Margolis. 2018. Solar plus: A review of the end-user economics of solar PV integration with storage and load control in residential buildings. *Applied energy* 228 (2018), 2165–2175.
[34] Tesla powerwall design. 2024. . https://www.tesla.com/powerwall
[35] Han Kun Ren, Malcolm Mcculloch, and David Wallom. 2022. Optimal sizing of solar photovoltaic and lithium battery storage to reduce grid electricity reliance in buildings.
[36] Recurrent Research. 2023. *Is your EV battery getting all the energy you pay for?*
[37] Masoume Shabani, Erik Dahlquist, Fredrik Wallin, and Jinyue Yan. 2020. Techno-economic comparison of optimal design of renewable-battery storage and renewable micro pumped hydro storage power supply systems: A case study in Sweden. *Applied Energy* 279 (2020), 115830.
[38] Solar.com. 2023. *Solar Panel Cost.* https://www.solar.com/learn/solar-panel-cost/
[39] UL Solutions. [n. d.]. *HOMER Software.* https://homerenergy.com
[40] Andreas Thingvad, Lisa Calearo, Peter Bach Andersen, and Mattia Marinelli. 2021. Empirical capacity measurements of electric vehicles subject to battery degradation from V2G services. *IEEE Transactions on Vehicular Technology* 70, 8 (2021), 7547–7557.
[41] Dai Wang, Jonathan Coignard, Teng Zeng, Cong Zhang, and Samveg Saxena. 2016. Quantifying electric vehicle battery degradation from driving vs. vehicle-to-grid services. *Journal of Power Sources* 332 (2016), 193–203.
[42] Hongxing Yang, Zhou Wei, and Lou Chengzhi. 2009. Optimal design and techno-economic analysis of a hybrid solar–wind power generation system. *Applied energy* 86, 2 (2009), 163–169.
[43] Bo Zhao, Xuesong Zhang, Peng Li, Ke Wang, Meidong Xue, and Caisheng Wang. 2014. Optimal sizing, operating strategy and operational experience of a stand-alone microgrid on Dongfushan Island. *Applied Energy* 113 (2014), 1656–1666.

Table 8: Experimental Parameters Used

Parameter	Value	Description
$a1_{\text{slope}}$	0.1920	Lower energy limit function.
$a2_{\text{slope}}$	-0.4865	Upper energy limit function.
η_c	0.9942	Charging efficiency of the stationary stationary battery.
η_d	1/0.9	Discharging efficiency of the stationary battery.
$V_{\text{nom,c}}$	3.8793	Nominal voltage during charging of the stationary battery
$V_{\text{nom,d}}$	3.5967	Nominal voltage during discharging of the stationary battery
η	100	Number of samples.
T_u	1h	Time unit.
U	0	Initial energy state of the stationary battery.
η_c^{ev}	0.935	Charging efficiency of the EV battery
η_d^{ev}	0.935	Discharging efficiency of the EV battery.

θ	HEMS	PV (kW)	Battery (kWh)	Cost ($)	Savings
0.8	N-U	1.96	1.77	3270	Baseline
	SG-U	1.91	1.48	3076	-6%
	SO-U	1.78	1.44	2893	-12%
	N-B	1.95	1.66	3209	-2%
	SG-B	1.69	1.01	2575	-21%
	SO-B	0.73	0.20	1010	-69%
0.5	N-U	4.29	10.57	10222	Baseline
	SG-U	4.23	10.28	10018	-2%
	SO-U	4.14	10.29	9905	-3%
	N-B	4.30	10.41	10169	-1%
	SG-B	4.16	2.55	6373	-38%
	SO-B	1.68	2.49	3242	-68%
0.2	N-U	7.38	25.26	20848	Baseline
	SG-U	7.32	24.93	20631	-1%
	SO-U	7.29	24.83	20540	-1.5%
	N-B	7.29	25.20	20718	-0.6%
	SG-B	7.49	12.61	15172	-27%
	SO-B	4.77	5.97	8717	-58%

Table 9: Sizing results obtained with SOPEVS for different θ values and operation policies for WFH T2 users and cost decrease compared to N-U.

θ	HEMS	PV (kW)	Battery (kWh)	Cost ($)	Savings
0.8	N-U	1.77	1.51	2912	Baseline
	SG-U	1.74	1.52	2875	-1%
	SO-U	1.73	1.51	2862	-2%
	N-B	1.76	1.40	2844	-2%
	SG-B	1.53	1.03	2388	-18%
	SO-B	0.97	1.30	1810	-38%
0.5	N-U	4.09	10.09	9762	Baseline
	SG-U	4.08	10.03	9716	-0%
	SO-U	4.03	10.14	9697	-1%
	N-B	4.05	9.81	9580	-2%
	SG-B	3.62	2.15	5515	-44%
	SO-B	3.07	2.23	4858	-50%
0.2	N-U	7.15	24.92	20405	Baseline
	SG-U	7.19	24.53	20274	-0.6%
	SO-U	7.14	24.83	20358	-0.2%
	N-B	7.21	24.24	20175	-1%
	SG-B	6.73	5.92	11141	-45%
	SO-B	6.12	5.47	10168	-50%

Table 10: Sizing results obtained with SOPEVS for different θ values and operation policies for WFH T3 users and cost decrease compared to N-U.

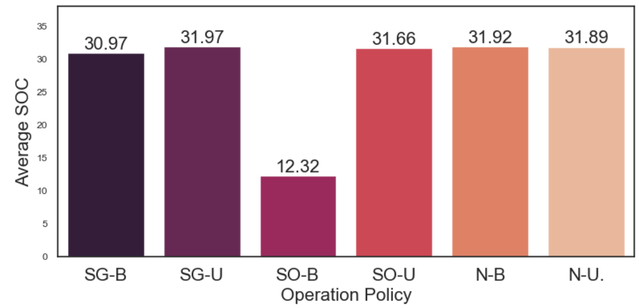

Figure 6: Average SOC at departure from home for T2 commuters and the different operation policies.

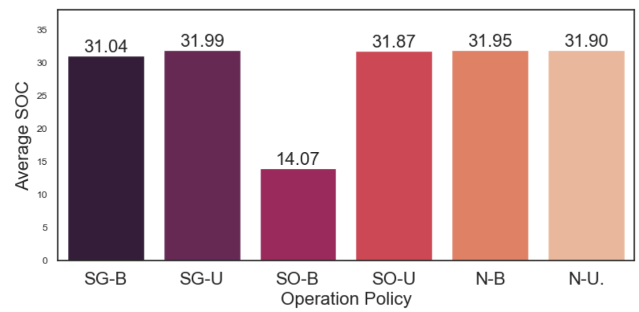

Figure 7: Average SOC at departure from home for T3 commuters and the different operation policies.